SOS1 and KSR1 modulate MEK inhibitor responsiveness to target resistant cell populations based on PI3K and KRAS mutation status

Brianna Daley*[1], Heidi M. Vieira*[2], Chaitra Rao[2, 3], Jacob Hughes[1], Dianna H. Huisman[2], Deepan Chatterjee[4], Nancy E. Sealover[1], Katherine Cox[1], James W. Askew[2], Robert A. Svoboda[5], Kurt W. Fisher[5], Robert E. Lewis[2#], and Robert L. Kortum[1#]

* These authors contributed equally to this paper

[1]Department of Pharmacology and Molecular Therapeutics, Uniformed Services University of the Health Sciences, Bethesda, MD

[2]Eppley Institute, Fred & Pamela Buffett Cancer Center, University of Nebraska Medical Center, Omaha, NE

[3]Current address: Wells Center for Pediatric Research, Indiana University School of Medicine, Indianapolis, IN

[4]Integrative Physiology and Molecular Medicine, University of Nebraska Medical Center, Omaha, NE

[5]Department of Pathology and Microbiology, University of Nebraska Medical Center, Omaha, NE

#Corresponding Authors

rlewis@unmc.edu

robert.kortum@usuhs.edu

Abstract

KRAS is the most commonly mutated oncogene; targeted therapies have been developed against mediators of key downstream signaling pathways, predominantly components of the RAF/MEK/ERK kinase cascade. Unfortunately, single-agent efficacy of these agents is limited both by intrinsic and acquired resistance. Survival of drug-tolerant persister cells within the heterogeneous tumor population and/or acquired mutations that reactivate RTK/RAS signaling can lead to outgrowth of tumor initiating cells (TICs) and drive therapeutic resistance. Here, we show that targeting the key RTK/RAS pathway signaling intermediates SOS1 or KSR1 both enhances the efficacy of and prevents resistance to the MEK inhibitor trametinib in *KRAS*-mutated lung and colorectal adenocarcinoma cell lines depending on the specific mutational landscape. The SOS1 inhibitor BI-3406 enhanced the efficacy of trametinib and prevented trametinib resistance by targeting TICs, but only in $KRAS^{G12}$- or $KRAS^{G13}$-mutated LUAD and COAD cell lines that lacked *PIK3CA* co-mutations. Cell lines with $KRAS^{Q61}$ and/or *PIK3CA* mutations were insensitive to combination therapy with trametinib and BI-3406. In contrast, deletion of the RAF/MEK/ERK scaffold protein *KSR1* prevented treatment-induced TIC upregulation and restored trametinib sensitivity across *KRAS* mutant cell lines in both *PIK3CA*-mutated and *PIK3CA* wildtype cancers. Our findings demonstrate that vertical targeting of RTK/RAS signaling is an effective strategy to target *KRAS*-mutated cancers, but the specific combination is dependent both on the specific KRAS mutant and underlying co-mutations. Thus, selection of optimal therapeutic combinations in KRAS-mutated cancers will require a detailed understanding of functional dependencies imposed by allele-specific KRAS mutations.

Significance Statement

Despite advances in the development of oncogene-targeted therapies, resistance invariably occurs. Therapeutic resistance is often due to the presence of intrinsic resistance or the outgrowth of tumor initiating cells, which results in the reactivation of the RTK/RAS pathway. Both dramatically reduce the number of effective treatment options available for patients. Combination therapy targeting up and downstream of RAS will delay the onset of resistance or prevent reactivation of the RTK/RAS pathway, prolonging the progression-free survival and overall survival of patients with lung and colon adenocarcinoma. To accomplish this, we have sought to understand the molecular characteristics of the cancer phenotypes that will most benefit from combination of MEK inhibition with either SOS1 inhibition with BI-3406, or KSR1 disruption by genomic deletion. We ultimately found that SOS1 inhibition increases the efficacy of, and prevents resistance to, Trametinib in $KRAS^{G12}$- and $KRAS^{G13}$-mutated LUAD and COAD cells without a *PIK3CA* co-mutation, while KSR1 disruption is effective across *KRAS* mutations, regardless of *PIK3CA* status.

Introduction

RAS proteins are encoded by three paralogs, KRAS, NRAS, and HRAS, which are, collectively, the most frequently mutated oncogene in cancer [1, 2]. Among those paralogs, KRAS is the most commonly mutated, found predominantly in pancreas adenocarcinoma (PDAC) (95%), lung adenocarcinoma (LUAD) (30-40%) and colorectal adenocarcinoma (COAD) (45-50%) [3]. KRAS is most commonly mutated at one of three mutational hotspots, G12, G13, or Q61 [4]; mutation of one of these sites alters KRAS GTP/GDP cycling leading to increased KRAS-GTP loading and activation. Within these specific codon mutations, there are differences in both nucleotide exchange and GTP hydrolysis which may have therapeutic implications [5]. While all three mutations reduce both the intrinsic GTPase activity of KRAS and GAP-mediated hydrolysis, Q61 mutants show dramatically reduced intrinsic hydrolysis compared to G12/G13 mutants [6, 7]. In contrast, G13 mutants show increased nucleotide exchange compared to G12 or Q61 mutants. While mutant KRAS has historically been considered undruggable, two inhibitors, sotorasib and adagrasib, have recently been developed and FDA approved to target $KRAS^{G12C}$ in non-small-cell lung cancer (NSCLC), representing a major breakthrough in the RAS targeting field [8, 9]. Targeted therapies have been developed against RAS effectors and mediators of key downstream signaling pathways, predominantly components of the RAF/MEK/ERK kinase cascade, including MEK inhibitors trametinib and selumetinib [10, 11].

Despite advances in these therapeutic interventions, treatment failure occurs due to resistance to oncogene-targeted therapies. Resistance can be classified as either intrinsic or acquired. Intrinsic resistance occurs due to the existence of tumor cells that have pre-existing resistance mechanisms to the chosen therapeutic method and are capable of persisting during therapeutic intervention [12]. Conversely, acquired resistance is often attributed to genomic instability and selective pressure for resistance-conferring mutations that promote outgrowth of these resistant cells [12, 13]. Mechanisms of acquired resistance to RTK signaling pathway inhibitors include alterations within KRAS or the activation of alternative RTKs that activate the

RTK/RAS pathway [14]. Resistance to targeted inhibitors also results from underlying tumor heterogeneity [15, 16]. Many tumors contain subpopulations of highly plastic cells with altered metabolic and drug efflux properties [17]. Also known as tumor initiating cells (TICs), these cell populations can serve as a sanctuary tumor population that expands during therapy, leading to treatment failure and recurrence [18]. Solid tumors are largely composed of non-TIC cells [18]. Targeted therapies developed to target these bulk non-TIC cells, allow the TIC populations to proliferate and differentiate post-therapy [18]. Turke et al., found that the use of MEK inhibition activated the PI3-kinase pathway, demonstrating its limited efficacy as a single-agent therapy [8, 19]. Targeted single-agent therapies, including the MEK inhibitor trametinib, enhance the TIC population through promotion of stem-like signaling pathways in colorectal cancer [20]. Phase II studies assessing the use of the MEK inhibitor selumetinib in combination with erlotinib, a first generation tyrosine kinase inhibitor of EGFR, showed similar results [8].

We propose that combination therapeutics that target both upstream and downstream signaling mediators can reduce upregulation of parallel signaling pathways. The RAS-GEF proteins, SOS1 and SOS2, regulate proximal RTK signaling. SOS1 inhibition has the potential to reduce activation of other RAS isoforms and prevent increased compensatory activation of PI3K. The SOS1 inhibitor, BI-3406, has shown efficacy in a pre-clinical study of NSCLC, COAD, and PDAC cells [21]. However, interactions with RAS-GEFs are dependent on the codon-specificity of the KRAS mutations. While each codon mutation has a defect in GAP-dependent hydrolysis, Q61-mutated RAS has an immense defect in intrinsic hydrolysis, cycling independently of RAS-GEFs [5]. Thus, selection of optimal therapeutic combinations for patients based on the mutational profile of their tumor requires a detailed understanding of the functional dependencies imposed upon RAS effectors and their downstream signaling pathways by the spectrum of allele-specific RAS mutations.

Combined therapeutics targeting parallel pathways can be limited by the development of toxicity. Combination of MEK and PI3K inhibitors in patients with advanced solid tumors led to the

development of dose-limiting toxicities [22]. Identifying mediators of RAS-dependent signaling or of parallel signaling pathways that are dispensable for the function of non-cancerous cells remains a challenge. The Kinase Suppressor of Ras (KSR) proteins are molecular scaffolds that mediate RAF/MEK/ERK signaling [23]. KSR1 has been found to be necessary for RAS-driven tumor formation, but dispensable for normal growth and development [23]. *ksr1*$^{-/-}$ mice are phenotypically normal but resistant to cancer formation [24, 25]. A recently developed inhibitor of KSR was found to increase the potency of MEK inhibitors, demonstrating that the use of KSR and MEK inhibitors may be a promising combination therapeutic strategy [26].

Therapeutic approaches should therefore address both intrinsic and acquired resistance through targeting upstream and downstream components of the signaling pathway and tumor heterogeneity by inhibiting stemness- and plasticity-promoting pathways. Thus, we propose that BI-3406 can be used to increase the efficacy of, and prevent resistance to, trametinib to limit intrinsic resistance and prevent the development of acquired resistance. Here, we show that disruption of either SOS1 signaling or the RAF/MEK/ERK scaffold KSR1, inhibits trametinib-induced TIC upregulation to prevent the development of trametinib resistance in LUAD and COAD cells. Our data show that SOS1 regulation of TICs and trametinib resistance is dependent on KRAS allelic substitution and *PIK3CA* mutational status, while KSR1 disruption is effective across KRAS mutations, regardless of *PIK3CA* status.

Results

SOS1 inhibition synergizes with trametinib to prevent rebound signaling in *KRAS^{G12}/PIK3CA^{WT}*-mutated LUAD cells. We previously showed that *SOS2* deletion reduced RTK-PI3K signaling and synergized with the MEK inhibitor trametinib to inhibit 3D growth of *KRAS*-mutated LUAD cells, however, the role of SOS1 was not assessed [27]. BI-3406 is a potent, selective SOS1 inhibitor previously shown to reduce 3D proliferation of *KRAS$^{G12/G13}$*-mutated, but not *KRAS^{Q61}*-mutated, cell lines as a single agent and to enhance the efficacy of trametinib in *KRAS*-mutated xenografts [21]. To characterize the extent to which BI-3406 enhances the effectiveness of trametinib, we treated a panel of 3D spheroid cultured *KRAS*-mutated LUAD cell lines with increasing doses of BI-3406 and/or trametinib in a 9x9 matrix of drug combinations and assessed for synergistic killing after 96 hours by Bliss Independence (Fig. 1A). We found that in *KRAS^{G12X}*-mutated cell lines H727 (G12V), A549 (G12S), and H358 (G12C), SOS1 inhibition markedly enhanced the efficacy of trametinib at or below the EC_{50} for trametinib (Fig. 1A) and showed a high excess over Bliss across the treatment matrix (Fig. 1B).

As a single agent, the effectiveness of trametinib is blunted by rapid induction of RTK/PI3K signaling followed by rebound ERK activation due, in part, to loss of ERK-dependent negative feedback signaling [19, 28, 29]. BI-3406 inhibited both trametinib-induced increase in PI3K/AKT activation and rebound ERK activation in *KRAS^{G12V}*-mutated H727 cells (Fig. 1C), suggesting that SOS1 inhibition blocks PI3K-dependent adaptive resistance to MEK inhibitors. Consistent with this hypothesis, SOS1 inhibition did not synergize with trametinib (Fig 1. A-B) or inhibit rebound signaling (Fig. S1) in *KRAS^{G12X}*-mutated LU99A cells that harbor a *PIK3CA* co-mutation, further enhancing the argument that SOS1 enhances trametinib efficacy by inhibiting RTK/PI3K rebound signaling. SOS1 inhibition also failed to synergize with trametinib (Fig. 1 A-B) and inhibit rebound signaling (Fig. S1) in four different *KRAS^{Q61}*-mutated LUAD cell lines regardless of *PIK3CA*

mutation status, confirming previous studies that SOS1 inhibition is only effective in *KRAS*-mutated cancer cells where KRAS cycles between the GTP and GDP-bound state [21].

Combination therapy with MEK and SOS1 inhibition targets trametinib-induced TIC outgrowth. Previous evidence has demonstrated that single agent therapy with EGFR Tyrosine Kinase Inhibitors resulted in increased TIC populations in NSCLC [30]. For the first time, we demonstrate that MEK inhibitors result in a similarly enhanced TIC population in *KRAS*-mutated LUAD cells. Using Aldefluor staining via flow cytometry, we demonstrate that two MEK inhibitors, trametinib and selumetinib, resulted in increased ALDH staining in H727 (G12V) (Fig. 2A), A549 (G12S) and H358 (G12C) (Fig. S2A) *KRAS*-mutated $PIK3CA^{WT}$ cells. Increased ALDH staining is indicative of an enhanced presence of TICs. However, to effectively confirm the presence of TICs, we used an Extreme Limiting Dilution Analysis (ELDA) to assess for spheroid growth using 96-well ultra-low attachment plates. This method is the true confirmatory test for determining the frequency of tumor initiating cells. Using the same three cell lines (H727, A549, H358), ELDAs were performed post-72 hours of MEK treatment and assessed 7-10 days later for TIC outgrowth. Comparable to our findings by Aldefluor staining, ELDA results demonstrated a significant increase in TIC frequency in MEK-inhibitor treated cells in comparison to untreated cells (Fig. 2B).

With previous evidence demonstrating that SOS1 inhibition was effective in blocking adaptive resistance and enhancing the efficacy of trametinib (Fig. 1C), we wanted to assess whether *SOS1* KO would be able to kill persister cells in *KRAS*-mutated LUAD cells. We discovered a marked decrease in TIC frequency in $KRAS^{G12X}$-mutated/$PIK3CA^{WT}$ *SOS1* KO cells compared to NT (Fig. 2C). We further show that SOS1 inhibition with BI-3406 decreases TIC frequency in a dose-dependent manner, with the greatest effect found at the highest dose in H727 (G12V) (Fig. 2D) and A549 (G12S) cells (Fig. S2B). Since SOS1 was required for TIC survival, we hypothesized that SOS1 inhibition would limit the survival of the increased TICs present following MEK inhibition with trametinib. To confirm, we pre-treated cells with two doses of

trametinib (Fig. 2E) and selumetinib (Fig. S2C) and used these cells for ELDAs plated with either media or BI-3406. We found that in H727, A549, and H358, SOS1 inhibition was able to target and significantly decrease the MEK-induced increase in TIC frequency (Fig. 2E and S2C). These findings support our hypothesis that BI-3406 can be used to enhance the efficacy of trametinib and prevent the development of resistance in the presence of *KRAS*$^{G12/G13}$-mutated LUAD cells without a *PIK3CA* mutation.

Unfortunately, we found that in *KRAS*^{G12X}/*PIK3CA*^{mut} (Lu99A) or in *KRAS*^{Q61X}-mutated cells that are either *PIK3CA* wildtype (Calu6) or *PIK3CA* mutant (H460), *SOS1* KO had no effect on TIC frequency (Fig. 2C). We further found that in the *KRAS*^{Q61K}/*PIK3CA*^{WT} Calu6 cells only, trametinib resulted in a significant increase in TIC frequency, while the presence of a *PIK3CA* co-mutation was sufficient to increase TIC frequency with no significant additional increase post-MEK inhibition (Fig. 2E). Of note, the H460 *KRAS*^{Q61H}/*PIK3CA*^{mut} cells are predominantly TIC in nature and, thus, the addition of MEK inhibitors would be unable to show any marked increase in TIC frequency (Fig. 2E). These findings suggest that the presence of mutations within the PI3K/AKT pathway is sufficient in driving the outgrowth of TICs.

***KSR1* KO restores trametinib responsiveness and inhibits TIC survival in *KRAS*-mutated LUAD genotypes.** Structural analysis of trametinib has revealed that it binds to the MEK-KSR complex [26]. The RAF/MEK/ERK scaffold protein, KSR1, is a positive regulator of ERK-dependent signaling in RAS-mutant cancers, but dispensable to the growth of untransformed cells and could therefore be a promising therapeutic target downstream of oncogenic RAS [23, 31, 32]. Thus, we next wanted to assess how *KSR1* KO could regulate TICs in trametinib resistant, *KRAS*^{Q61X}-mutated LUAD cells or those with a *PIK3CA* co-mutation where SOS1 inhibition was rendered ineffective. We generated *KSR1* KO by CRISPR/Cas9 in two mutationally distinct LUAD cell lines, A549 (*KRAS*^{G12S}/*PIK3CA*^{WT}) and H460 (*KRAS*^{Q61H}/*PIK3CA*^{mut}). We found that *KSR1* KO A549 cells exhibit significantly diminished *in vitro* clonogenicity and completely depleted ALDH enzyme activity which indicates a decrease in TICs; both effects could be rescued by addback of

the KSR1 transgene (Fig. 3A-B). We next performed *in vivo* ELDAs to quantify the KSR1 effect on the proportion of TICs and found that *KSR1* KO A549 cells demonstrated X-fold reduction in TIC frequency relative to non-targeting control cells, an effect that was restored by KSR1 addback (Fig. 3C *Placeholder for A549 in vivo ELDA repeat*). *KSR1* KO also sensitized A549 cells to trametinib (Fig. 3E), mirroring the effects of SOS1 inhibition on trametinib sensitivity in the context of $KRAS^{G12S}$-genotype.

In $KRAS^{Q61}$/$PIK3CA^{mut}$ cells, in which RAS cycles independently of SOS, SOS1 inhibition does not synergize with trametinib (Fig. 1A-B) or suppress TICs (Fig. 2E). We sought to determine whether inhibition of signaling downstream of RAS via KSR1 disruption affects TIC survival and trametinib sensitivity in $KRAS^{Q61H}$/$PIK3CA^{mut}$ H460 LUAD cells. CRISPR/Cas9-mediated knockout of *KSR1* reduced TIC-frequency 4-fold by *in vivo* limiting dilution analysis, demonstrating that KSR1 regulates the TIC population even in the context of this genotype (Fig. 3D). Dose-response curves with H460 demonstrate that *KSR1* KO also sensitizes H460 cells to trametinib (Fig. 3F-G) and selumetinib (Fig. 3SA-B) under both 2D (adherent) and 3D (spheroid) culture conditions. These data demonstrate that inhibition of RTK signaling distal to RAS by *KSR1* KO depletes TICs and restores trametinib responsiveness even in the context of Q61 *RAS*-mutant and *PIK3CA*-mutant LUAD cells, where proximal RTK signaling inhibition with BI-3406 fails to deplete TICs or synergize with trametinib.

In COAD, *KSR1* KO prevents trametinib-induced TIC increase regardless of PIK3CA mutational status. While *PIK3CA*/*KRAS* co-mutations are relatively rare in LUAD, they commonly co-occur in COAD, with approximately one third of *KRAS*-mutated COADs harboring co-existing *PIK3CA* mutations. We sought to test the extent to which the *KRAS/PIK3CA* genotype sensitivity to SOS1 and *KSR1* ablation we observed in LUAD would remain true in COAD. Therefore, we generated CRISPR/Cas9-mediated knockout of *KSR1* in four COAD cell lines with varying *PIK3CA* status: SW480 ($KRAS^{G12C}$/$PIK3CA^{WT}$) LoVo ($KRAS^{G13D}$/$PIK3CA^{WT}$), LS174T

(*KRAS*^{G12D}/*PIK3CA*^{mut}), and T84 (*KRAS*^{G13D}/*PIK3CA*^{mut}). *In vitro* ELDAs performed with *KSR1* KO in the four COAD cell lines demonstrated a 2-3 fold decrease in TIC-frequency compared to NT cells. Further, *KSR1* KO prevented the trametinib-induced increase in TIC in the four COAD cell lines (Fig. 4), demonstrating that the KSR1 effect on TICs in COAD is independent of *PIK3CA* mutational status. Further, treatment with BI-3406 in NT cells prevented trametinib-induced TIC increase in the cell lines with wildtype *PI3KCA* status (SW480 and LoVo), but not in *PI3KCA*^{mut} cell lines (LS174T and T84), consistent with our LUAD findings (Fig. 2E). In *KSR1* KO cells, combination of trametinib with BI-3406 did not further affect TIC frequency, concordant with SOS1 acting upstream of KSR1 in the RTK/Ras pathway.

KSR1 regulation of TIC survival in *KRAS*-mutated COAD is dependent on interaction with ERK. KSR1 mediates ERK-dependent signaling in transformed and untransformed cells via direct interaction between its DEF domain and ERK [33-35]. We sought to determine whether interaction with ERK was necessary for KSR1 regulation of tumor initiating cells in COAD. A KSR1 transgene deficient in binding ERK due to engineered mutation in the DEF-domain, KSR1-AAAP, was expressed in *KSR1* KO colorectal adenocarcinoma cell line HCT116 (Fig. 5A). Expression of KSR1-AAAP in *KSR1* KO cells failed to rescue ALDH activity, single cell clonogenicity, or anchorage-independent growth by soft agar assay to the level observed with wildtype KSR1 addback, demonstrating the necessity of ERK interaction on KSR1 regulation of TICs (Fig. 5B-D). To assess our findings in a translational setting, an *in vivo* limiting dilution analysis was performed. Notably, a 70-fold decrease in the proportion of TICs was found in the *KSR1* KO cells compared to those with NT cells, demonstrating the significant impact of KSR1 on TICs in COAD (Fig. 5E).

SOS1 inhibition prevents trametinib resistance in *PIK3CA*^{WT} *KRAS*$^{G12/13}$-mutated cells, while *KSR1* KO prevents trametinib resistance in *PIK3CA*^{mut} cells across KRAS allelic

substitutions. To assess the effect of SOS1 and KSR1 disruption on outgrowth of trametinib-resistant cells, we utilized multi-well resistance assays in which cells are grown on a 96-well plate and treated either with trametinib alone or in combination with BI-3406. Wells are scored twice weekly to assess for 50% confluency or more to determine the presence of resistance. Of the five LUAD cell lines tested, SOS1 inhibition with BI-3406 prevented outgrowth of trametinib-resistant cells in (*KRAS*^{G12V}/*PI3KCA*^{WT}) and H358 cells (*KRAS*^{G12C}/*PI3KCA*^{WT}), but not in LUAD cell lines with either a *PIK3CA* co-mutation (LU99A), *KRAS*^{Q61} mutation (Calu6), or both (H460) (Fig. 6A-E). In contrast, *KSR1* KO was able to prevent outgrowth of trametinib-resistant cells in H460 LUAD cells (Fig. 6F) and in the HCT116 COAD cell line (*KRAS*^{G13D}/*PIK3CA*^{mut}) (Fig. 6G). To determine whether interaction with ERK was necessary for the KSR1 effect on trametinib resistance, we further tested whether expression of the ERK-binding mutant KSR1^{AAAP} transgene in *KSR1* KO cells could rescue trametinib-resistant outgrowth. KSR1^{AAAP} partially restored outgrowth relative to *KSR1* KO cells while wildtype KSR1 completely restored outgrowth (Fig. 6F), suggesting KSR1 interaction with ERK affects trametinib resistance but may be occurring in combination with other KSR1-dependent effects.

Discussion

With the rapid development of resistance to common therapeutic modalities in both NSCLC and COAD, current guidelines strongly advise molecular analysis at the time of diagnosis to develop personalized care for each patient [12, 36]. This personalized care includes targeted therapy with either single agent use or combination therapy, the latter of which has shown to be more beneficial for increasing overall survival and progression-free survival in patients with *KRAS*-mutated malignancies. Evidence shown here demonstrates single agent therapy with the MEK inhibitor, trametinib, results in the rapid acquisition of resistance through reactivation of the RTK pathway and subsequent positive selection of tumor initiating cells. Throughout this study, we use several experimental methods to comprehensively study how combination therapy through MEK inhibition and either SOS1 or KSR1 disruption can be used to target PC- and TIC-dependent resistance development based on oncogene mutational profile.

While combination therapy can provide synergistic therapeutic effects with the potential to reduce effective clinical doses of each component drugs, combined therapeutics targeting parallel pathways can still be limited by the development of toxicity, as evidenced by clinical trials of combined MEK and PI3K inhibition in solid tumors [22]. We used Bliss Independence analysis to determine the lowest dose of both trametinib and BI-3406 that, in combination, provided the highest degree of killing in *KRAS*-mutated LUAD cells. Using this synergistic matrix allowed each subsequent experiment to be translationally focused for future clinical importance. With the main clinical concern of resistance, we used rebound signaling studies to assess the presence and impact of MEK inhibition alone and in combination with BI-3406 in our *KRAS*-mutated LUAD cell lines. The upregulation of both the MEK/ERK and PI3K/AKT pathways within 48 to 72 hours of treatment initiation demonstrated that cancer cells were already resistant to MEK inhibition. However, SOS1 inhibition in addition to trametinib was sufficient to prevent rebound signaling, indicating this combination therapy can successfully counteract intrinsic resistance in a cancer cell population.

To understand the foundation of resistance in our *KRAS*-mutated LUAD and COAD cells, we used the mainstay of stem cell analysis, Extreme Limiting Dilution Analysis (ELDA). We found that pre-treatment with trametinib alone resulted in increased frequency of resistant cells as indicated by enhanced spheroid growth in the ELDA assay. This growth was prevented in cells treated with BI-3406 post-trametinib therapy, indicating SOS1 inhibition targeted resistant cells while simultaneously accentuating the killing effect of trametinib. While ELDAs lack the ability to differentiate between intrinsic and acquired resistance mechanisms, these data implicate the expansion of resistant cells with enhanced TIC capacity, as a potential cause for therapeutic failure of trametinib treatment.

The heterogeneous molecular behavior of codon-specific mutations in *KRAS*-mutated malignancies provides additional complexity to targeting efforts [5]. We determined that in *KRAS*-mutated LUAD cells with a G12 or G13 allelic substitution, the SOS1 inhibitor BI-3406 can prevent the resistant cell selective process. In contrast, SOS1 and MEK inhibition used in combination was unsuccessful when tested in *KRAS*-mutated LUAD cell lines with a Q61 allelic substitution since these cells are RAS-GEF independent. Western blot analysis and ELDA assays demonstrate that SOS1 inhibition is insufficient in blocking RTK reactivation and resistance. Further, *KRAS*-mutated LUAD cell lines with a *PIK3CA* co-mutation, regardless of its codon specificity, were resistant to proximal RTK inhibition with BI-3406 and MEK inhibition since there is constitutively active PI3K pathway signaling. Most interesting, we found that *KRAS*-mutated cells with a Q61 allelic substitution and a *PIK3CA* co-mutation have an innately high level of TICs, rendering them insensitive to the TIC-inducing effect of MEK inhibition. This is in comparison to other cell lines that either have a G12 or G13 allelic substitution but are *PIK3CA* mutated or Q61 cells that are *PIK3CA* WT, all conditions that demonstrate increased frequency of TICs with trametinib.

To address the inconsistent responses to combination therapy with trametinib and BI-3406 in select oncogenic mutations, we turned to investigate an additional, potentially targetable

effector of RAS-dependent signaling, the RAF/MEK/ERK scaffold, KSR1. Trametinib is a unique MEK inhibitor that binds at the MEK-KSR complex, suggesting co-targeting of KSR1 with trametinib may have unique synergistic effects [32, 37]. We used *KSR1* KO models to assess the effectiveness of trametinib +/- *KSR1* disruption in molecular conditions where combination of trametinib and BI-3406 was shown to be ineffective. Indeed, we found that *KSR1* KO cells had significantly decreased TIC frequency at baseline and were resistant to the trametinib-induced TIC expansion in these cells, across *KRAS* allelic substitutions tested and in *PIK3CA*-mutant cells. Kortum and Lewis previously demonstrated phosphorylation of AKT to be unaffected by *KSR1* KO in MEFS [31, 38]. That *KSR1* KO was effective at regulating TICs in all cell lines tested, regardless of *PIK3CA* mutation, suggests *KSR1*-dependent signaling either converges to regulate pathway mediators downstream of PI3K/AKT, or promotes TIC function through pathways distinct from, and not compensated by, the level of PI3K/AKT signaling.

To assess the effect of these combination therapies in a translational setting, *in vitro multi-well r*esistance assays were used to assess the development of acquired resistance. We found that in $KRAS^{G12}$-mutated LUAD cell lines that were *PIK3CA* wildtype, SOS1 and MEK inhibition prevented the development of resistance through targeting both persistent cell populations and preventing the outgrowth of tumor initiating cells. Further, complete *KSR1* KO resulted in similar targeting of resistant cell populations in all tested cell lines regardless of codon or *PIK3CA* mutation status.

Our finding that the ERK-binding mutant $KSR1^{AAAP}$ fails to rescue TIC properties and trametinib resistance to the extent of rescue by wildtype KSR1 implicates ERK-dependent signaling in KSR1 regulation of TICs and trametinib resistance. This finding is consistent with KSR1 function as a RAF/MEK/ERK scaffold, and with previous findings implicating ERK in KSR1-dependent downstream effects [23, 34, 39, 40]. Intriguingly, the ERK-binding mutant KSR1 transgene does partially rescue trametinib-resistant colony outgrowth by multi-well resistance assay relative to *KSR1* KO cells. The moderate effect seen by $KSR1^{AAAP}$ in this setting indicates

that KSR1 regulation of trametinib resistance may be partially due to the unique nature of trametinib interaction with the MEK-KSR complex, or additional, non ERK-mediated KSR1-dependent effects. KSR1 has been shown to interact with metabolic regulator AMP kinase (AMPK) [41], and KSR1-dependent regulation of AMPK has been shown to play a pro-tumorigenic role in COAD through promotion of oxidative metabolic effectors and CRC survival [42, 43]. Future research efforts should outline the role of KSR1 interaction with AMPK on regulation of tumor-initiating cells and trametinib resistance.

Overall, our study provides evidence that treatment failure is due to the development of resistance because of either persistent or tumor initiating cells. The complete molecular mechanisms of BI-3406 and KSR1 regulation of resistant cell populations have yet to be elucidated. Preliminary data indicate BI-3406 may be halting growth and proliferation of these persister cells. Our findings using the ERK-binding mutant KSR1 transgene indicate ERK as a proximal effector of KSR1 effect on TICs but suggest additional mechanisms may also play a role. Future experiments are necessary to further explore the respective signaling pathways involved in SOS1 and KSR1 regulation of tumor initiating cells.

Nonetheless, evidence presented here demonstrates that BI-3406, a SOS1 inhibitor, or KSR1 disruption by genomic KO, can increase the efficacy of trametinib while preventing both intrinsic and acquired resistance from developing. Combination therapy with BI-3406 and Trametinib was shown to be most effective in patient populations with *KRAS*^{G12}- or *KRAS*^{G13}-mutated, *PIK3CA* wildtype, LUAD or COAD cells. Ultimately, our study advances understanding of RAS effector targeting based on allele-specific RAS mutations and specific oncogene driver profiles, and emphasizes the need for in-depth molecular characterization of each patient's tumor to select optimal therapeutic combinations.

Materials and Methods

Cell culture

Lung and colon cancer cell lines were purchased from ATCC or JCRB (LU99A). After receiving the cells, they were expanded and frozen at passage 3 and 4; cell were passaged once they became 70-80% confluent and maintained in culture for 2-3 months before thawing a new vial as prolonged passaging can alter TIC frequency [44]. Cell lines were cultured at 37°C and 5% CO2. Cells were passaged in either RPMI [H727, A549, H358, LU99A, H460] or DMEM [Calu6, H650, H1155, SW620, SW480, LS174T, LoVo, T84, HCT116] supplemented with 10% FBS and 1% penicillin/streptomycin. For signaling experiments, cells ere seeded in 24-well micropatterned AggreWell 400 low-attachment plates (StemCell) at 9 x 10^5 cells/ well in 2 mL of medium. 24-h post plating, 1 mL of media was replaced with 2 x inhibitor. Cells were treated with inhibitor for 0 – 72 hours; for all treatments >24-h, half of the media was removed and replaced with fresh 1 x inhibitor daily.

Production of recombinant lentiviruses and sgRNA studies

Lentiviruses were produced by co-transfecting MISSION lentiviral packaging mix (Sigma) into 293 T cells using Mirus TransIT-Lenti transfection reagent (Mirus Bio # MIR6605) in Opti-MEM (Thermo Scientific #31-985-062). At 48 hr post-transfection, viral supernatants were collected and filtered. Viral supernatants were then either stored at -80°C or used immediately to infect cells in combination with polybrene at 8 mg/mL.

Generation of pooled genomic *SOS1* KO cell lines: For *SOS1* KO studies, cells were infected with lentiviruses based on pLentiCRISPRv2 with either a non-targeting sgRNA (NT; CCATATCGGGGCGAGACATG) or a sgRNA targeting SOS1 (SOS1-2; GCATCCTTTCCAGTGTACTC) [45]. 48 hr post-infection, cells were selected in 4 mg/mL

Puromycin (Invitrogen). 7-10 days after selection, cells were analyzed for SOS1 or KSR1 expression. Cell populations showing >80% deletion were used for further study.

Generation of clonal genomic *KSR1* KO cell lines: sgRNA sequences targeting KSR1 or non-targeting control were inserted into pCAG-SpCas9-GFP-U6-gRNA (Addgene #79144, gift of Jizhong Zou). PEI transfection was used to insert pCAG-SpCas9-GFP-U6-sgKSR1 or non-targeting control into A549, H460, and HCT116 cells. GFP-selection by fluorescence-activated cell sorting was performed 48 hours post-transfection, and colonies were grown out with the use of cloning rings.

Generation of pooled genomic *KSR1* KO cell lines: sgRNA sequences targeting KSR1 or non-targeting control were inserted into pLentiCRISPRv2GFP (Addgene #82416). The constructs were PEI transfected into HEK293T cells along with psPAX2 lentiviral packaging construct (Addgene #12259) and pMD2.G envelope construct (Addgene #12259). Lentivirus-containing media was harvested at 96 hours, and added to SW480, LoVo, LS174T and T84 cells. GFP+ cells were selected by fluorescence-activated cell sorting.

Generation of KSR1 addback in genomic *KSR1* KO cell lines: Murine KSR1 was cloned into MSCV-IRES -RFP. MSCV-IRES-KSR1-RFP and MSCV-IRES-KSR1-GFP (Addgene #25973) were PEI transfected into HEK293T cells along with pUMVC retroviral packaging construct (Addgene # 8449) and VSVG envelope construct (Addgene #8454). Lentivirus-containing media was harvested at 96 hours, and added to clonal KSR1 KO HCT116, A549, and H460 cells (MSCV-IRES-KSR1-GFP-containing virus), and pooled KSR1 KO SW480, LoVo, LS174T and T84 cells

(MSCV-IRES-KSR1-RFP-containing virus). GFP- or RFP-selection, respectively, was performed by fluorescence-activated cell sorting 48 hours post-transfection.

Single Cell Colony-forming Assay: Cells were DAPI-stained for viability determination and live cells were single cell sorted as one cell per well into a 96-well, U-bottom, non-adherent plate (Takara Bio). Cells were grown for 14 days, after which colony formation was determined using Cell Titer Glo® viability assay (Promega) performed according to manufacturer instructions.

Flow cytometry

Cells were plated in 10 or 6 cm tissue-culture treated plates and allowed to adhere for 24-48 hours prior to drug treatmentOnce cells were 50-75% confluent, cells were treated with the indicated concentration of tramentinib or selumetinib for 72 hours. After 72-h treatment, cells were harvested by trypsinization, spun down, resuspended in Aldefluor Assay Buffer (StemCell) at $1*10^6$ cells/mL, and stained for ALDH activity using the Aldefluor Assay Kit per manufacturer's instructions. An aliquot of cells was pre-treated with the ALDH inhibitor DEAB, which inhibits used as a negative gating control. Data was analyzed using FloJo with and are presented as the % of cells showing aldeflour staining (and thus ALDH activity) over DEAB controls.

Soft Agar Colony-forming Assay: $1x10^3$ cells per dish were plated onto 35mm dishes in 0.4% NuSieve Agarose (Lonza #50081). Six replicates of each condition were plated. At 14 days, colony formation was assessed by counting colonies > 100μM in their largest diameter.

Cell lysis and Western blotting

Cells were lysed in RIPA buffer (1% NP-40, 0.1% SDS, 0.1% Na-deoxycholate, 10% glycerol, 0.137 M NaCl, 20 mM Tris pH [8.0], protease (Biotool #B14002) and phosphatase (Biotool #B15002) inhibitor cocktails) for 20 min at 4°C and spun at 10,000 RPM for 10 min. Clarified lysates were boiled in SDS sample buffer containing 100 mM DTT for 10 min prior to western blotting. Proteins were resolved by sodium dodecyl sulfate-polyacrylamide (Criterion TGX precast) gel electrophoresis and transferred to nitrocellulose membranes. Western blots were developed by multiplex Western blotting using anti-SOS1 (Santa Cruz sc-256; 1:500), anti-b-actin (Sigma AC-15; 1:5,000 or Santa Cruz Biotechnology sc-47778, 1:2000 dilution), anti-a-tubulin (Abcam ab89984 1:2000); anti-pERK1/2 (Cell Signaling 4370; 1:1,000), anti-ERK1/2 (Cell Signaling 4696; 1:1000), anti-pAKT Ser473 (Cell Signaling 4060; 1:1000), anti-AKT (Cell Signaling 2920; 1:1000), anti-KSR1 (Abcam ab68483, 1:750 dilution), primary antibodies. Anti-mouse, anti-rabbit, and anti-chicken secondary antibodies conjugated to IRDye680 or IRDye800 (LI-COR; 1:20,000) were used to probe primary antibodies. Western blot protein bands were detected and quantified using the Odyssey system (LI-COR).

Extreme Limiting Dilution Assays (ELDA)

In vivo: In equal volumes of 50% Cultrex® Basement Membrane Extract (R&D Systems) 50% Dulbecco's Modified Eagle Medium (Cytiva), dilutions ranging from 5 to 1000 cells were injected subcutaneously into the shoulder and hip of 6-8-week old triple immunodeficient male NOD-Prkdc^{em26Cd52}Il2rg^{em26Cd22}/NjuCr (NCG, Charles River) mice. Mice were monitored for tumor formation by palpation. Once tumor sized reached 1cm^3, mice were sacrificed, tumors were excised and the number of tumors formed entered into online ELDA calculator [46] to determine TIC frequency.

In situ : TIC frequency was assessed by in situ ELDA assay. Cells were seeded in 96-well ultra-low attachment flat bottomed plates (Corning Corstar #3474) at decreasing cell concentrations (1000 cells well – 1 cell /well) at half log intervals (1000, 300, 100, 30, 10, 3, 1), 12 wells per

condition with the exception of the 10 cells/well condition, for which 24 wells were seeded. Cells were cultured for 7-10 days, and wells with spheroids > 100 mM were scored as spheroid positive. TIC frequency and significance between groups was calculated by ELDA website https://bioinf.wehi.edu.au/software/elda/. [47]. To assess the effect of trametinib on TIC frequency, cells were left untreated or were pre-treated with the indicated dose of trametinib or selumetinib for 72-h, after which cells were rested for 48-72 hours prior to plating. To assess the effect of SOS1 inhibition, cells were seeded +/- 300 nM BI-3406.

Bliss Independence Analysis for Synergy

Cells were seeded at 750 cells per well in 100 mL in the inner-60 wells of 96-well ultra-low attachment round bottomed plates (Corning #7007) or Nunc NucleonSphera microplates (ThermoFisher # 174929) and allowed to coalesce as spheroids for 24–48 hr prior to drug treatment. Cells were treated with drug for 96 hr prior to assessment of cell viability using CellTiter-Glo 2.0. For all studies, outer wells (rows A and H, columns 1 and 12) were filled with 200 mL of PBS to buffer inner cells from temperature and humidity fluctuations. Triplicate wells of cells were then treated with increasing concentrations trametinib alone, BI-3406 alone, or the combination of trametininb + BI-3406 in a 9x9 matrix of drug combinations on a similog scale for 72 (adherent cultures) or 96 (spheroids) hr. Cell viability was assessed using CellTiter-Glo 2.0 (30 mL/well). Luminescence was assessed using a Bio-Tek Cytation five multi-mode plate reader. Data were normalized to the maximum luminescence reading of untreated cells, and individual drug EC50 values were calculated using Prism9 by non-linear regression using log(inhibitor) vs. response. For all drug-treatment studies, the untreated sample for each cell line was set to 100%. This would mask any differences in 3D cell proliferation seen between cell lines. Excess over Bliss was calculated as the Actual Effect – Expected Effect as outlined in [45]. The SUM EOB is calculated by taking the sum of excess over bliss values across the 9 x 9 treatment matrix. EOB values > 0 indicate increasing synergy.

Resistance Assays

Cells were plated at low density (250 cells/well) in replicate 96-well plates, and each plate was treated with the indicated doses of trametinib +/- BI-3406. Wells were fed and assessed weekly for outgrowth, wells that were > 50% confluent were scored as resistant to the given dose of trametinib. Data are plotted as a Kaplan-Meyer survival curve; significance was assessed by comparing Kaplan-Meyer curves using Prism 9.

List of Key Resources:

KSR1 antibody: Abcam ab68483, 1:750 dilution
β-actin antibody: Santa Cruz Biotechnology sc-47778, 1:2000 dilution
β-actin antibody: Sigma AC-15; 1:5,000 dilution
SOS1 antibody: Santa Cruz sc-256; 1:500 dilution
a-tubulin antibody: Abcam ab89984 1:2000 dilution
pERK1/2 antibody: Cell Signaling 4370; 1:1,000 dilution
ERK1/2 antibody: Cell Signaling 4696; 1:1000 dilution
pAKT Ser473 antibody: (Cell Signaling 4060; 1:1000 dilution
AKT antibody: Cell Signaling 2920; 1:1000 dilution
KSR1 sgRNA sequences:
CR1 5' TTGGATGCGCGGCGGGAAAG 3'
CR2 5' CTGACACGGAGATGGAGCGT 3'
NT sgRNA sequence: 5' CCATATCGGGGCGAGACATG 3'
SOS1 sgRNA sequence: 5' GCATCCTTTCCAGTGTACTC 3'
Plasmid catalog numbers listed in the sections above.

Acknowledgements. We thank the UNMC Cell Analysis Facility and UNMC Animal Facility. **Funding**: This work was supported by funding from the NIH (R01 CA255232 and R21 CA267515 to R.L.K and P20 GM121316 to R.E.L), the CDMRP Lung Cancer Research Program (LC180213 to R.L.K. and LC210123 to R.E.L and R.L.K.), and a CRADA from Boehringer Ingelheim (to R.L.K). The funders had no role in the study design, data collection and interpretation, or the decision to submit the work for publication. The opinions and assertions expressed herein are those of the authors and are not to be construed as reflecting the views of Uniformed Services

University of the Health Sciences or the United States Department of Defense. **Competing interests:** The Kortum laboratory receives funding from Boehringer Ingelheim to study SOS1 as a therapeutic target in RAS-mutated cancers.

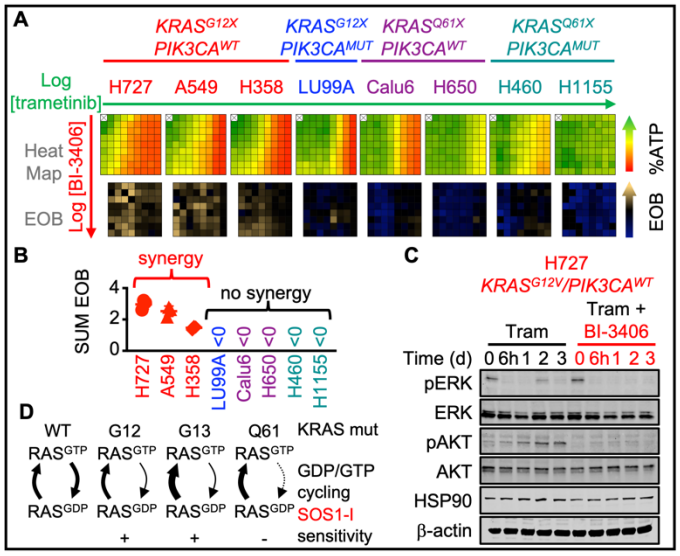

Figure 1. MEK and SOS1 inhibition synergize to prevent rebound signaling in *KRAS^{G12}/PIK3CA^{WT}*-mutated LUAD cells.

(A) Heat map of cell viability (top) and excess over Bliss (EOB, bottom) for the indicated *KRAS*-mutated LUAD cell lines treated with increasing (similog) doses of trametinib ($10^{-10.5}$ – 10^{-7}), BI-3406 (10^{-9} – $10^{-5.5}$) or the combination of trametinib + BI-3406 under 3D spheroid culture conditions. The *KRAS* and *PIK3CA* mutational status of each cell line are indicated. Data are the mean from three independent experiments, each experiment had three technical replicates.

(B) The sum of excess over Bliss for the 9×9 matrix of trametinib + BI3406 treatments from **A**. EOB > 0 indicates increasing synergy.

(C) Western blots of WCLs of 3D spheroid cultured H727 cells treated with trametinib (10 nM) +/- BI-3406 (300 nM) for the indicated times. Western blots are for pERK, ERK, pAKT (Ser 473), AKT, HSP90, and β-actin.

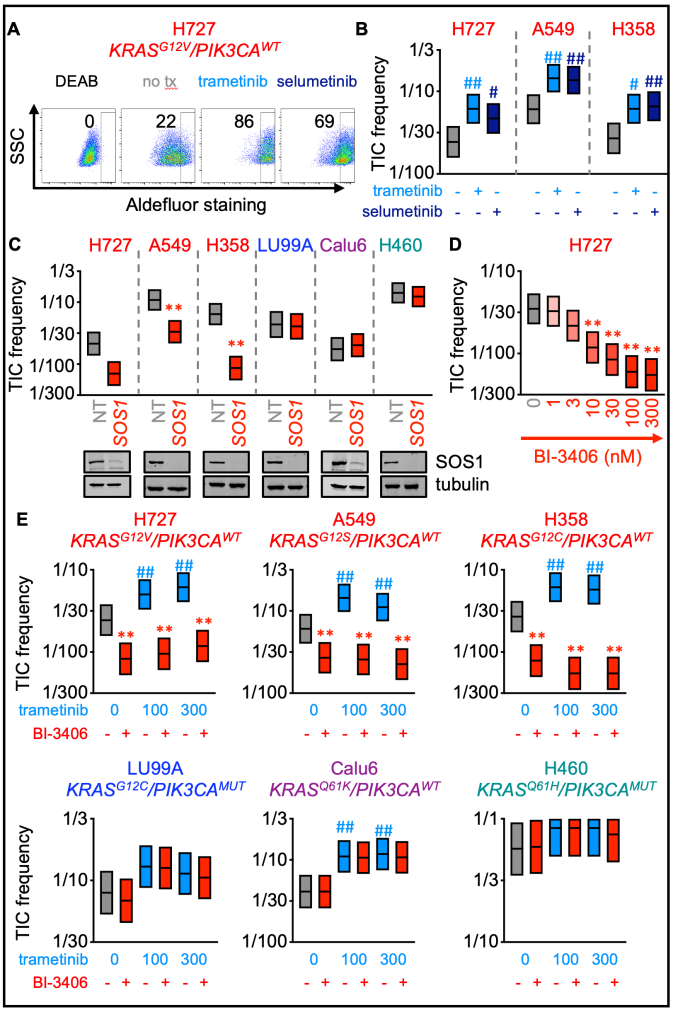

Figure 2. SOS1 inhibition prevents trametinib-induced TIC outgrowth.
(A) Aldefluor staining for ALDH enzyme activity in DEAB negative control (DEAB), untreated H727 cells, or H727 cells treated with 100 nM trametinib or selumetinib for 72 hours. **(B)** TIC frequency from in situ ELDAs of the indicated cell lines pre-treated with 100 nM trametinib or selumetinib for 72 hours. # $p < 0.05$ vs untreated; ## $p<0.01$ vs. untreated for TIC upregulation.
(C) TIC frequency from in situ ELDAs (top) and Western blotting of WCLs for SOS1 and tubulin in the indicated LUAD cell lines where *SOS1* has been knocked out vs. non-targeting controls. ** $p<0.01$ vs. untreated. **(D)** TIC frequency from in situ ELDAs of H727 cells treated with the indicated doses of BI-3406.
(E) TIC frequency from in situ ELDAs of the indicated cell lines pre-treated with trametinib for 72 hours to upregulate TICs, and then left untreated or treated with BI-3406.
# $p < 0.05$ vs untreated; ## $p<0.01$ vs. untreated for TIC upregulation by MEK inhibitor treatment vs. untreated controls. * $p < 0.05$ vs untreated; ** $p<0.01$ for TIC inhibition by BI-3406 treatment compared to untreated controls.
Data are representative from three independent experiments.

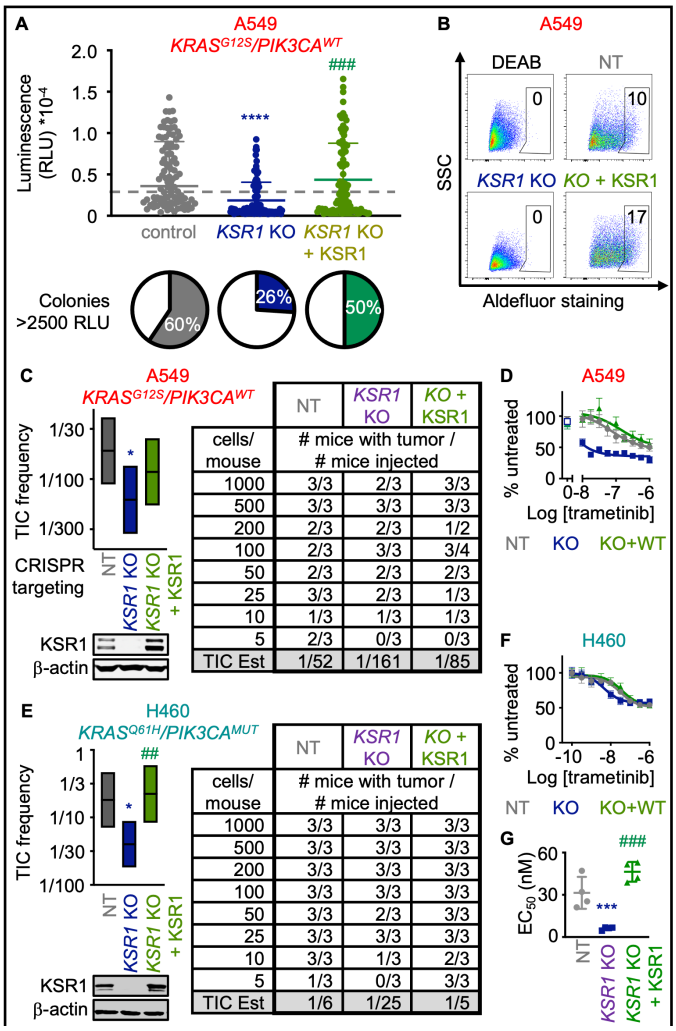

Figure 3. *KSR1* KO inhibits tumor initiating cell (TIC) survival and enhances sensitivity to trametinib in *KRAS*-mutated LUAD genotypes.

(A-D) Assays in A549 (*KRAS*^{G12S}/*PIK3CA*^{WT}) NT, *KSR1* KO, and *KSR1* KO+*KSR1* cells. **(A)** Single cell colony forming assays. Cells were single cell plated in non-adherent conditions, and colony formation was scored at 14 days by CellTitre Glo. Each individual point represents a colony. **(B)** Aldefluor staining for ALDH enzyme activity above in DEAB negative control. (**C)** *In vivo* limiting dilution analysis data showing TIC frequency The indicated numbers of cells were injected into the shoulder and flank of NCG mice (Charles River). Tumors were scored at 30 days. **(D)** Trametinib dose response curve indicating % cell viability for cells treated with the indicated concentrations of trametinib in anchorage-dependent (2D) conditions for 72 hours. Western blotting for KSR1 and b-actin in each cell population are shown in **C.**

(E-G) Assays in H460 (*KRAS*^{Q61H}/*PIK3CA*^{MUT}) NT, *KSR1* KO, and *KSR1* KO+*KSR1* cells. **(E)** *In vivo* limiting dilution analysis data showing TIC frequency The indicated numbers of cells were injected into the shoulder and flank of NCG mice (Charles River). Tumors were scored at 30 days. **(F-G).** Trametinib dose response curve indicating % cell viability (F) and EC50 values (G) for cells treated with the indicated concentrations of trametinib in anchorage-dependent (2D) conditions for 72 hours. Western blotting for KSR1 and b-actin in each cell population are shown in **E.**

*p < 0.05; **** p<0.001 vs non-targeting controls; # p<0.05, ## p<0.01 vs. *KSR1* KO.

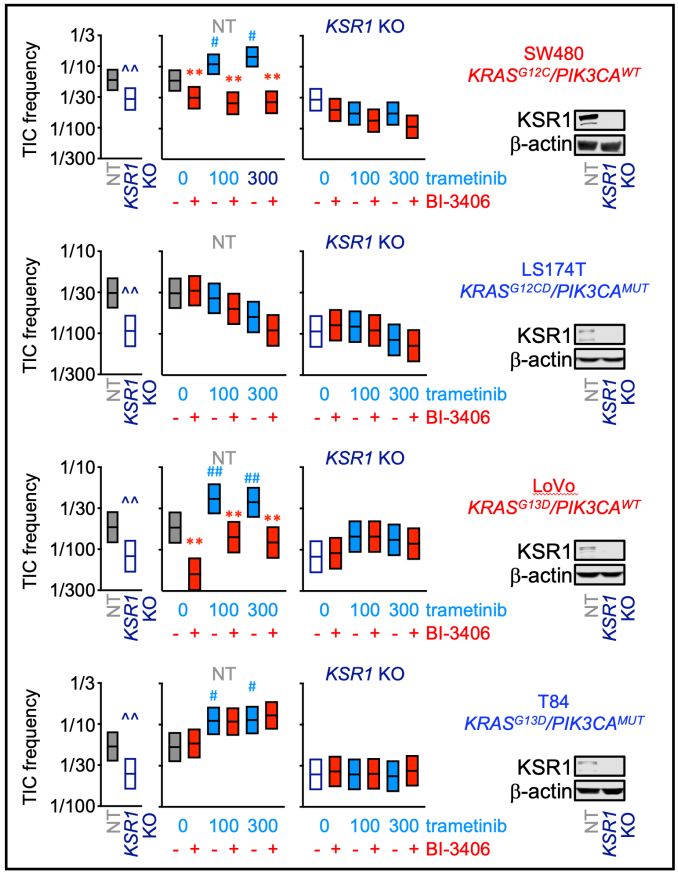

Figure 4. *KSR1* KO and SOS1 inhibition show differential inhibition of basal and trametinib-induced TICs in *KRAS*-mutated COAD cells.

TIC frequency from in situ ELDAs of the indicated NT and *KSR1* KO COAD cells pre-treated with trametinib for 72 hours to upregulate TICs, and then left untreated or treated with the SOS1 inhibitor BI-3406. The *KRAS* and *PIK3CA* mutational status for each cell line is indicated. Western blots of WCLs for KSR1 and β-actin are shown on the right.
^^ $p < 0.01$ for KSR1 KO vs non-targeting control.
# $p < 0.05$ vs untreated; ## $p<0.01$ vs. untreated for TIC upregulation by MEK inhibitor treatment vs. untreated controls.
** $p<0.01$ for TIC inhibition by BI-3406 treatment compared to untreated controls.
Data are representative from three independent experiments.

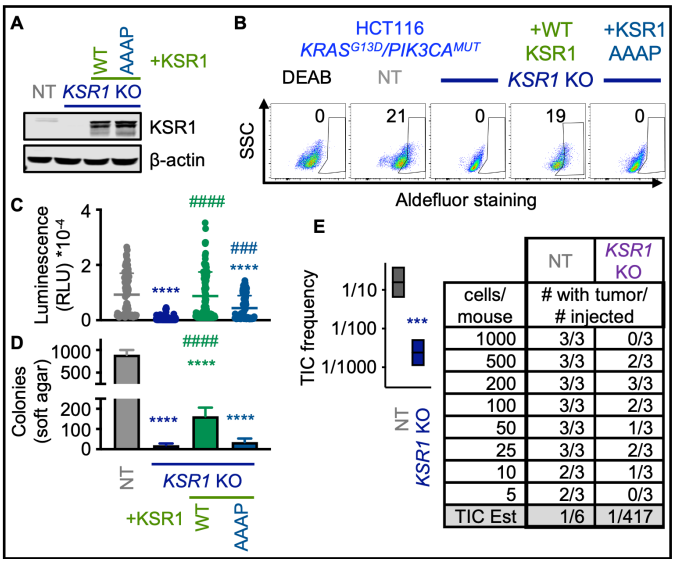

cells/ mouse	NT # with tumor/ # injected	KSR1 KO # with tumor/ # injected
1000	3/3	0/3
500	3/3	2/3
200	3/3	3/3
100	3/3	2/3
50	3/3	1/3
25	3/3	2/3
10	2/3	1/3
5	2/3	0/3
TIC Est	1/6	1/417

Figure 5. KSR1 regulation of TICs in COAD is dependent on interaction with ERK and relevant *in vivo*.

(A-D) Assays in HCT116 (*KRAS*^{G13D}*/PIK3CA*^{mut} NT, *KSR1* KO, *KSR1* KO + *KSR1* addback, and *KSR1* KO+ERK-binding mutant KSR1 (KSR1^{AAAP}) addback cells.

(A) Western blot for KSR1 and β-actin loading controls from WCLs. **(B)** Aldefluor staining for ALDH enzyme activity above in DEAB negative control. **(C)** Single cell colony forming assays. Cells were single cell plated in non-adherent conditions, and colony formation was scored at 14 days by CellTitre Glo. Each individual point represents a colony. **(D)** Soft agar colony forming assay. 1x10^3 cells per well were plated in 0.4% agar, and colony formation was scored at 14 days. **(E)** *In vivo* limiting dilution analysis data showing frequency of TICs in Non-targeting Control (NT) and KSR1 KO HCT116 COAD cells. The indicated numbers of cells were injected into the shoulder and flank of NCG mice (Charles River). Tumors were scored at 30 days.

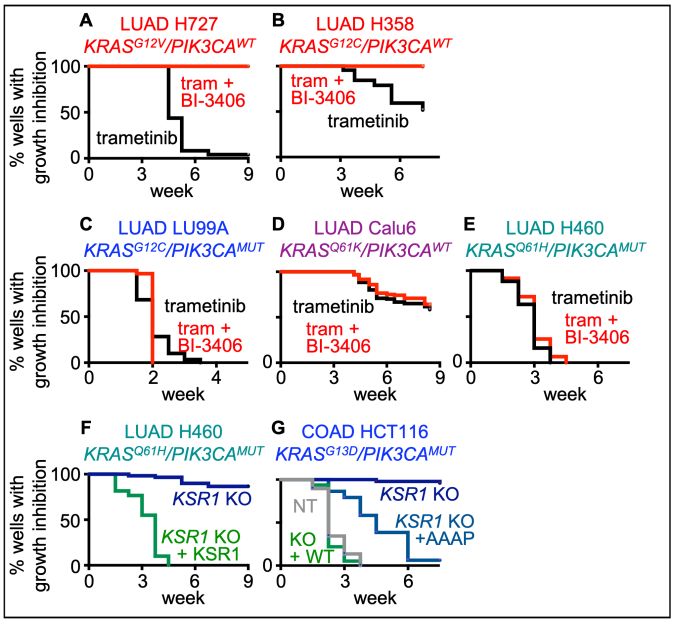

Figure 6 SOS1 inhibition and *KSR1* KO delay outgrowth of trametinib-resistant cell in multi-well resistance assays depending on the KRAS mutational status.

The indicated *KRAS*-mutated cell lines were plated at low density (250 cells/well) in replicate 96-well plates, and each plate was treated with the indicated dose of osimertinib. Wells were fed and assessed weekly for outgrowth, wells that were > 50% confluent were scored as resistant to the given dose of trametinib-resistant. Curves depict percent of wells with inhibited growth. Data are plotted as a Kaplan-Meyer survival curve.
(A-E). SOS1 inhibition using BI-3406 inhibited trametinib resistance in *KRAS*^{G12X}-mutated/*PIK3CA*^{WT} H727 **(A)** and H358 **(B)** LUAD cells to 30 nM trametinib, but not in *KRAS*^{G12X}-mutated/*PIK3CA*^{MUT} LU99A cells to 30 nM trametinib **(C),** *KRAS*^{Q61X}-mutated Calu6 cells to 30 nM trametinib **(D),** or H460 cells to 1 μM trametinib **(E)**.
(F-G). *KSR1* KO iinhibited trametinib resistance in *KRAS*^{Q61K}-mutated/*PIK3CA*^{MUT} H460 LUAD cells to 1 μM trametinib **(F)** and *KRAS*^{G13D}-mutated/*PIK3CA*^{MUT} HCT116 COAD cells to 30 nM trametinib **(G).** In **G,** a WT KSR1 transgene fully restored trametinib sensitivity to *KSR1* KO , whereas cells expressing the ERK-binding mutant KSR1^{AAAP} showed delayed, but not inhibited, trametinib resistance.

References

1. Cox, A.D., et al., *Drugging the undruggable RAS: Mission Possible?* Nature Reviews Drug Discovery, 2014. **13**(11): p. 828-851.
2. Prior, I.A., F.E. Hood, and J.L. Hartley, *The Frequency of Ras Mutations in Cancer.* Cancer Res, 2020. **80**(14): p. 2969-2974.
3. Reck, M., et al., *Targeting KRAS in non-small-cell lung cancer: recent progress and new approaches.* Annals of Oncology, 2021. **32**(9): p. 1101-1110.
4. Bear, A.S., et al., *Biochemical and functional characterization of mutant KRAS epitopes validates this oncoprotein for immunological targeting.* Nature Communications, 2021. **12**(1).
5. Sealover, N.E. and R.L. Kortum, *Heterogeneity in RAS mutations: One size does not fit all.* Sci Signal, 2022. **15**(746): p. eadc9816.
6. Hunter, J.C., et al., *Biochemical and Structural Analysis of Common Cancer-Associated KRAS Mutations.* Mol Cancer Res, 2015. **13**(9): p. 1325-35.
7. Smith, M.J., B.G. Neel, and M. Ikura, *NMR-based functional profiling of RASopathies and oncogenic RAS mutations.* Proc Natl Acad Sci U S A, 2013. **110**(12): p. 4574-9.
8. Uprety, D. and A.A. Adjei, *KRAS: From undruggable to a druggable Cancer Target.* Cancer Treatment Reviews, 2020. **89**: p. 102070.
9. Tang, D., G. Kroemer, and R. Kang, *Oncogenic KRAS blockade therapy: renewed enthusiasm and persistent challenges.* Molecular Cancer, 2021. **20**(1).
10. Ciombor, K.K. and T. Bekaii-Saab, *Selumetinib for the treatment of cancer.* Expert Opin Investig Drugs, 2015. **24**(1): p. 111-123.
11. Wright, C.J.M. and P.L. McCormack, *Trametinib: First Global Approval.* Drugs, 2013. **73**(11): p. 1245-1254.
12. Delahaye, C., et al., *Early Steps of Resistance to Targeted Therapies in Non-Small-Cell Lung Cancer.* Cancers (Basel), 2022. **14**(11).
13. Cabanos, H.F. and A.N. Hata, *Emerging Insights into Targeted Therapy-Tolerant Persister Cells in Cancer.* Cancers (Basel), 2021. **13**(11).
14. Awad, M.M., et al., *Acquired Resistance to KRAS^{G12C} Inhibition in Cancer.* New England Journal of Medicine, 2021. **384**(25): p. 2382-2393.
15. Dawood, S., L. Austin, and M. Cristofanilli, *Cancer stem cells: implications for cancer therapy.* Oncology (Williston Park), 2014. **28**(12): p. 1101-7, 1110.
16. Meador, C.B. and A.N. Hata, *Acquired resistance to targeted therapies in NSCLC: Updates and evolving insights.* Pharmacol Ther, 2020. **210**: p. 107522.
17. Batlle, E. and H. Clevers, *Cancer stem cells revisited.* Nature Medicine, 2017. **23**(10): p. 1124-1134.
18. Shibue, T. and R.A. Weinberg, *EMT, CSCs, and drug resistance: the mechanistic link and clinical implications.* Nature Reviews Clinical Oncology, 2017. **14**(10): p. 611-629.
19. Turke, A.B., et al., *MEK inhibition leads to PI3K/AKT activation by relieving a negative feedback on ERBB receptors.* Cancer Res, 2012. **72**(13): p. 3228-37.
20. Zhan, T., et al., *MEK inhibitors activate Wnt signalling and induce stem cell plasticity in colorectal cancer.* Nature Communications, 2019. **10**(1): p. 2197.
21. Hofmann, M.H., et al., *BI-3406, a Potent and Selective SOS1-KRAS Interaction Inhibitor, Is Effective in KRAS-Driven Cancers through Combined MEK Inhibition.* Cancer Discov, 2021. **11**(1): p. 142-157.
22. Grilley-Olson, J.E., et al., *A phase Ib dose-escalation study of the MEK inhibitor trametinib in combination with the PI3K/mTOR inhibitor GSK2126458 in patients with advanced solid tumors.* Invest New Drugs, 2016. **34**(6): p. 740-749.

23. Kortum, R.L. and R.E. Lewis, *The Molecular Scaffold KSR1 Regulates the Proliferative and Oncogenic Potential of Cells.* Molecular and Cellular Biology, 2004. **24**(10): p. 4407-4416.
24. Lozano, J., et al., *Deficiency of Kinase Suppressor of Ras1 Prevents Oncogenic Ras Signaling in Mice.* Cancer Research, 2003. **63**(14): p. 4232-4238.
25. Nguyen, A., et al., *Kinase suppressor of Ras (KSR) is a scaffold which facilitates mitogen-activated protein kinase activation in vivo.* Mol Cell Biol, 2002. **22**(9): p. 3035-45.
26. Dhawan, N.S., A.P. Scopton, and A.C. Dar, *Small molecule stabilization of the KSR inactive state antagonizes oncogenic Ras signalling.* Nature, 2016. **537**(7618): p. 112-116.
27. Sheffels, E., et al., *Oncogenic RAS isoforms show a hierarchical requirement for the guanine nucleotide exchange factor SOS2 to mediate cell transformation.* Sci Signal, 2018. **11**(546).
28. Fedele, C., et al., *SHP2 Inhibition Prevents Adaptive Resistance to MEK Inhibitors in Multiple Cancer Models.* Cancer Discov, 2018. **8**(10): p. 1237-1249.
29. Ahmed, T.A., et al., *SHP2 Drives Adaptive Resistance to ERK Signaling Inhibition in Molecularly Defined Subsets of ERK-Dependent Tumors.* Cell Rep, 2019. **26**(1): p. 65-78 e5.
30. Codony-Servat, J., et al., *Cancer Stem Cell Biomarkers in EGFR-Mutation-Positive Non-Small-Cell Lung Cancer.* Clin Lung Cancer, 2019. **20**(3): p. 167-177.
31. Kortum, R.L., et al., *The molecular scaffold kinase suppressor of Ras 1 is a modifier of RasV12-induced and replicative senescence.* Mol Cell Biol, 2006. **26**(6): p. 2202-14.
32. Gonzalez-Del Pino, G.L., et al., *Allosteric MEK inhibitors act on BRAF/MEK complexes to block MEK activation.* Proceedings of the National Academy of Sciences, 2021. **118**(36): p. e2107207118.
33. McKay, M.M., D.A. Ritt, and D.K. Morrison, *Signaling dynamics of the KSR1 scaffold complex.* Proceedings of the National Academy of Sciences, 2009. **106**(27): p. 11022-11027.
34. Kortum Robert, L., et al., *The Molecular Scaffold Kinase Suppressor of Ras 1 Is a Modifier of RasV12-Induced and Replicative Senescence.* Molecular and Cellular Biology, 2006. **26**(6): p. 2202-2214.
35. Cacace Angela, M., et al., *Identification of Constitutive and Ras-Inducible Phosphorylation Sites of KSR: Implications for 14-3-3 Binding, Mitogen-Activated Protein Kinase Binding, and KSR Overexpression.* Molecular and Cellular Biology, 1999. **19**(1): p. 229-240.
36. Alexander, M., S.Y. Kim, and H. Cheng, *Update 2020: Management of Non-Small Cell Lung Cancer.* Lung, 2020. **198**(6): p. 897-907.
37. Khan, Z.M., et al., *Structural basis for the action of the drug trametinib at KSR-bound MEK.* Nature, 2020. **588**(7838): p. 509-514.
38. Kortum, R.L. and R.E. Lewis, *The molecular scaffold KSR1 regulates the proliferative and oncogenic potential of cells.* Mol Cell Biol, 2004. **24**(10): p. 4407-16.
39. McCall, J.L., et al., *KSR1 and EPHB4 Regulate Myc and PGC1β To Promote Survival of Human Colon Tumors.* Mol Cell Biol, 2016. **36**(17): p. 2246-61.
40. Rao, C., et al., *KSR1- and ERK-dependent translational regulation of the epithelial-to-mesenchymal transition.* eLife, 2021. **10**: p. e66608.
41. Costanzo-Garvey, D.L., et al., *KSR2 Is an Essential Regulator of AMP Kinase, Energy Expenditure, and Insulin Sensitivity.* Cell Metabolism, 2009. **10**(5): p. 366-378.
42. Fisher Kurt, W., et al., *AMPK Promotes Aberrant PGC1β Expression To Support Human Colon Tumor Cell Survival.* Molecular and Cellular Biology, 2015. **35**(22): p. 3866-3879.

43. Fisher, K.W., et al., *Kinase suppressor of ras 1 (KSR1) regulates PGC1α and estrogen-related receptor α to promote oncogenic Ras-dependent anchorage-independent growth.* Mol Cell Biol, 2011. **31**(12): p. 2453-61.
44. Qureshi-Baig, K., et al., *Tumor-Initiating Cells: a criTICal review of isolation approaches and new challenges in targeting strategies.* Molecular Cancer, 2017. **16**(1).
45. Theard, P.L., et al., *Marked synergy by vertical inhibition of EGFR signaling in NSCLC spheroids shows SOS1 is a therapeutic target in EGFR-mutated cancer.* Elife, 2020. **9**.
46. Hu, Y. and G.K. Smyth, *ELDA: Extreme limiting dilution analysis for comparing depleted and enriched populations in stem cell and other assays.* Journal of Immunological Methods, 2009. **347**(1): p. 70-78.
47. Hu, Y. and G.K. Smyth, *ELDA: extreme limiting dilution analysis for comparing depleted and enriched populations in stem cell and other assays.* J Immunol Methods, 2009. **347**(1-2): p. 70-8.